

# Parent phases of doped Mott insulators: a Cluster DMFT study

J.-C. Domenge\* and G. Kotliar

Department of Physics and Astronomy and Center for Condensed Matter Theory,  
Rutgers University, Piscataway, NJ 08854-8019

(Dated: August 18, 2008)

We investigate the insulating phases of a frustrated Hubbard model in its strong coupling regime at half-filling. We pay special attention to all the symmetry breaking instabilities that can be described by Dynamical Mean Field Theory (DMFT) on a square plaquette. We identify several mean-field solutions, two Néel states breaking the  $SU(2)$  symmetry, a dimer phase and a Mott insulator which doesn't break any symmetry. The singlet to singlet fluctuations soften dramatically in the latter phase, giving rise to dimerization fluctuations as well as chiral fluctuations that are both low-lying. We present a simple picture of the different DMFT states and their evolution with frustration.

Frustrated two dimensional Mott insulators are interesting in their own right, and are realized in Helium films as well as in transition metal and organic compounds. They received enormous attention, following the discovery of superconductivity in copper oxide based materials and the suggestion [1] that the phenomenon of high temperature superconductivity is connected to the doping of a "spin liquid", namely a Mott insulator without magnetic long range order at zero temperature.

In this line of thought one would like to understand spin liquids, metals and their relation to superconducting states, within one same framework. Many insights into this problem were obtained using mean field methods such as slave boson mean field theory and the large-N expansion. [2] More recently the development of Dynamical Mean Field Theory (DMFT) and its cluster extensions [3, 4, 5, 6] have improved the description of the unusual electronic structure of strongly correlated materials. Indeed this approach applied to simple models accounts for many properties of both the  $d$ -wave superconducting state and the normal state of copper oxides [7, 8] and  $\kappa$ -organics. [9]

In this letter, we make a general mean-field ansatz to study symmetry-breaking solutions describing the insulating phases of the half-filled  $t_1 - t_2$  Hubbard model at large  $U$ , using cluster DMFT on a  $2 \times 2$  plaquette. We identify several Mott insulating phases and we take advantage of the substantial simplifications provided by the CDMFT method to obtain a simple understanding of their local properties. Such a program was carried out for the anisotropic triangular lattice in Ref. 9, while in Refs. 10, 11 DMFT methods were applied to the Mott insulating regime on the kagomé lattice. Unlike the above studies, however, our DMFT ansatz is compatible with dimerization, a common instability in frustrated spin systems.

We start with a frustrated Hubbard model on the square lattice

$$\mathcal{H} = - \sum_{(i,j),\sigma} (t_{ij} c_{i\sigma}^\dagger c_{j\sigma} + h.c.) + U \sum_i n_{i\uparrow} n_{i\downarrow} - \mu \sum_{i,\sigma} n_{i\sigma} \quad (1)$$

where  $c_{i\sigma}$  (resp.  $c_{i\sigma}^\dagger$ ) destroys (resp. creates) an electron

at site  $i$  with spin projection  $\sigma$  on the  $z$ -axis,  $t_{ij} = t_1$  (resp.  $t_2$ ) for pairs  $(i,j)$  of NN (resp. NNN), and  $t_{ij} = 0$  otherwise.  $U$  is the onsite Coulomb repulsion and  $\mu$  is the chemical potential.

We investigate the insulating phases of (1) at half-filling using Cellular DMFT on a  $2 \times 2$  plaquette. To be more specific, we consider the following Anderson Impurity Model

$$\begin{aligned} \mathcal{H}_{\text{AIM}} = \mathcal{H}|_{\square} &+ \sum_{(\alpha,\beta),\sigma} (\epsilon_{\alpha\beta,\sigma} a_{\alpha\sigma}^\dagger a_{\beta\sigma} + h.c.) \\ &+ \sum_{(i,\alpha),\sigma} (V_{i\alpha,\sigma} c_{i\sigma}^\dagger a_{\alpha\sigma} + h.c.) \end{aligned} \quad (2)$$

where  $\mathcal{H}|_{\square}$  is the restriction of the original Hamiltonian (1) to one plaquette  $\square$  (the impurity), and the last two terms read the kinetic energy of the conduction bath and the hybridization between the bath and the plaquette, respectively. In substance, solving the self-consistent Cellular DMFT equations amounts to finding a set of bath parameters  $\{\epsilon_{\alpha\beta,\sigma}, V_{i\alpha,\sigma}\}_{\alpha,\beta,\sigma}$  that mimic the influence of the infinite square lattice surrounding plaquette  $\square$  in the original model (1). [3]

On the technical side, the use of Exact Diagonalization to obtain the ground state of (2) severely constrains the size of the bath (8 sites in the present study). Further, numerical tractability requires that the total number of bath parameters be even more limited, usually by imposing additional symmetry relations among them. This step requires extra care, especially when investigating possible symmetry-breaking instabilities. Indeed, there is no *spontaneous* symmetry breaking in a finite system, hence the symmetry of the ground state of (2) is merely that of the Hamiltonian itself. Finally, attention must also be paid to the CDMFT self-consistency condition. The latter describes the embedding of the impurity plaquette  $\square$  in the infinite lattice, which must be compatible with the symmetry of the thermodynamic ground state. These points will be discussed at greater length elsewhere. [12]

We first present the mean-field ground states of (1) at half-filling and for large  $U$ : in the following  $t_1 = 1$  and

$U = 16$ . We have checked that this  $U$  puts the system well within the Mott insulating phase. In this regime the cost of double occupancy is avoided through the coherent hopping of two or more electrons, and to lowest order in  $t_{1,2}/U$ , (1) reduces to the  $J_1 - J_2$  Heisenberg model, with  $J_i = 4t_i^2/U(1 + \mathcal{O}((t/U)^2))$ . [12] Hence the meaningful frustration parameter is  $(t_2/t_1)^2$ . For finite  $U$ , higher order processes also contribute and generate longer exchange loops, starting with four-spins exchange at order  $t_i^4/U^3$ .

Figure 1 shows the evolution of three order parameters on the impurity upon increasing the frustration ratio  $t_2/t_1$ . First, the usual Néel order is detected by computing the normalized staggered magnetization  $\langle m_{\mathbf{k}_I} \rangle = \frac{2}{N_c} \sum_{i \in \square} e^{i\mathbf{k}_I \cdot \mathbf{r}_i} \langle S_i^z \rangle$ , where  $\mathbf{k}_I = (\pi, \pi)$  and  $N_c = 4$ . Another Néel order is anticipated at large frustration from previous studies of the closely-related  $J_1 - J_2$  model (see Ref. 13 and references therein). It corresponds to the entropic selection of one of the two degenerate impurity momenta  $\mathbf{k}_I = (0, \pi)$  and  $(\pi, 0)$ . Finally we compute  $\langle D \rangle = \langle \mathbf{S}_2 \cdot \mathbf{S}_3 - \mathbf{S}_1 \cdot \mathbf{S}_2 \rangle$  which evidences the  $x - y$  symmetry breaking of the spin correlations. Note that  $\langle D \rangle$  is non-zero if the impurity plaquette carries singlets on parallel NN bonds, but also for the  $(0, \pi)$  and  $(\pi, 0)$  Néel orders. Hence the dimerization itself is detected through both i)  $\langle D \rangle \neq 0$  and ii)  $\langle m_{(0,\pi)} \rangle = \langle m_{(\pi,0)} \rangle = 0$ .

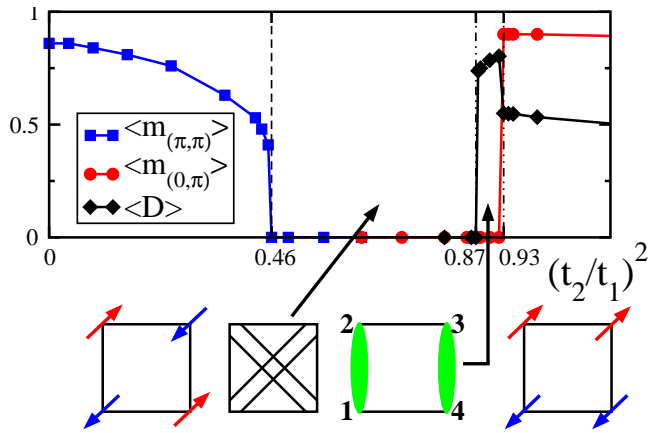


FIG. 1: (Color online) Evolution of the Néel and dimer order parameters computed on the impurity plaquette for increasing frustration  $t_2/t_1$  (see text). Cartoon pictures of the various phases on the impurity plaquette are shown: in both Néel phases the relative orientation of the spins is indicated, while in the paramagnetic phases, triplets and singlets are pictured with parallel lines and green ellipses, respectively.

At  $t_2 = 0$  we recover the  $(\pi, \pi)$  Néel order with a staggered magnetization renormalized to about 86% of its classical value. Upon increasing the frustration,  $\langle m_{(\pi,\pi)} \rangle$  is increasingly renormalized until quantum fluctuations completely wipe out the Néel order at  $(t_2/t_1)^2 \simeq 0.46$ .

For  $0.46 \lesssim (t_2/t_1)^2 \lesssim 0.87$  the ground state is a sin-

glet formed by the four-spins of the impurity. Since it doesn't break the point symmetry of a square, we will refer to it as a fully symmetric paramagnet in the following. For  $0.87 \lesssim (t_2/t_1)^2 \lesssim 0.93$  the ground state is still paramagnetic (all Néel order parameters are zero) but it spontaneously breaks the rotational symmetry of the lattice and dimerizes in an almost pure product of singlets on the plaquette, as evidenced by  $D \simeq 3/4$ .

Finally  $SU(2)$  spontaneously breaks again for  $(t_2/t_1)^2 \gtrsim 0.93$  where the  $(0, \pi)$  Néel phase kicks in through a first-order transition, as suggested by the abrupt increase of  $\langle m_{(0,\pi)} \rangle$  jumping from 0 to about 90% of its classical value. This is further supported by the simultaneous existence of two solutions to the CDMFT equations in this region, namely the fully symmetric paramagnet and the  $(0, \pi)$  Néel order. [12]

*Interpretation* Cellular DMFT provides a local picture of each of the phases of model (1), in terms of the states of the self-consistent impurity model (2).

In semi-classical phases, such as the  $(\pi, \pi)$  Néel phase at small  $t_2$ , tracing out the bath degrees of freedom results in a reduced density matrix for the impurity plaquette that has most of its weight in one state of the plaquette. This state resembles a classical, antiferromagnetic, spin configuration dressed by quantum fluctuations. The orientation of the spin is picked up by the self-consistent Weiss field.

To gain more insight into the fully symmetric phase that takes over at intermediate frustration  $0.46 \lesssim (t_2/t_1)^2 \lesssim 0.87$ , we investigate the nature of the two lowest eigenstates of the impurity model, noted  $|0\rangle$  and  $|1\rangle$ . From each one of these states we construct the reduced "density matrix" of the impurity, defined by  $\rho_I^\alpha = \text{Tr}_B |\alpha\rangle\langle\alpha|$  where  $\alpha = 0, 1$  and  $\text{Tr}_B$  denotes the partial trace over the bath degrees of freedom. The spectral decomposition of the operators  $\rho_I^\alpha$  reveals that most of the weight ( $\sim 95\%$ ) is carried by a single state of the plaquette noted  $|\alpha\rangle_I$ , *i.e.*  $\rho_I^\alpha \simeq |\alpha\rangle_I \cdot \langle I|\alpha|$ . This means that  $|\alpha\rangle \simeq |\alpha\rangle_I |\alpha\rangle_B$ , *i.e.* the impurity and the bath are only weakly entangled in the subspace spanned by  $|0\rangle$  and  $|1\rangle$ , at stark contrast with the situation in single-site DMFT.

Further, the nature of the impurity states  $|\alpha\rangle_I$  provide a simple mean-field picture of the paramagnetic phases and their evolution with  $t_2/t_1$ . Namely, in the fully symmetric phase,  $|0\rangle_I$  is the singlet obtained by adding two triplets along the diagonals (1,3) and (2,4) of the plaquette, noted  $|\boxtimes\rangle$ , only lightly dressed by quantum fluctuations. Similarly,  $|1\rangle_I$  is the product of two diagonal singlets, noted  $|\boxtimes\rangle$ .

We will show that the disappearance of the fully symmetric paramagnet at  $(t_2/t_1)^2 \simeq 0.87$  is driven by the closing of the gap between these two singlets. We believe that this is the *local* mean-field description of the abundance of low-lying singlets commonly observed at Quantum Phases Transition points in frustrated quantum magnets. [13] This is supported by the observation

that the two impurity singlets are orthogonal  $\langle \boxtimes | \boxtimes \rangle = 0$ , and span exactly the two-dimensional subspace of the half-filled impurity with total spin  $S_I = 0$ . Hence, within plaquette DMFT there is simply no additional, linearly independant, half-filled impurity singlet susceptible to condense.

When the singlet gap closes, the zero-energy subspace is enlarged to  $\{|\boxtimes\rangle, |\boxtimes\rangle\}$ . Increasing the frustration in  $0.87 \lesssim (t_2/t_1)^2 \lesssim 0.93$  lifts this degeneracy and selects a particular direction within this subspace, either  $|\square\rangle = \sqrt{3}/2|\boxtimes\rangle + 1/2|\boxtimes\rangle$ , or  $|\square\rangle = \sqrt{3}/2|\boxtimes\rangle - 1/2|\boxtimes\rangle$ .

*Dynamical singlet correlations* More insight into the paramagnetic phases can be gained by considering higher-order spin correlations. Indeed, in a seminal paper [14] Wen discussed a particular class of spin liquids, breaking both Parity (P) and Time reversal (T), whose order parameter is the scalar chirality  $\langle E_{ijk} \rangle = \langle \mathbf{S}_i \cdot \mathbf{S}_j \times \mathbf{S}_k \rangle$ . The relevance of these chiral spin liquids for the  $J_1 - J_2$  model was claimed by the author, on the premise that the coherence in the collective dynamics of three spins on a plaquette is generally enhanced by a non-zero  $J_2$ , possibly to the point where  $\langle E_{ijk} \rangle \neq 0$ . Beyond the original mean-field study by Wen, an early numerical work of the  $J_1 - J_2$  model evidenced the softening of chiral fluctuations, although no long-range chiral order was found. [15] Within the CDMFT treatment of the related Hubbard model (1), the weak entanglement between the bath and the impurity yields  $\langle 0 | E_{ijk} | 0 \rangle \simeq \langle \boxtimes | E_{ijk} | \boxtimes \rangle$  in the fully symmetric phase. Consider for instance the triplet (1, 2, 3) of impurity sites. Direct computation shows that  $E_{123}|\boxtimes\rangle = i\sqrt{3}/4|\boxtimes\rangle$  and  $E_{123}|\boxtimes\rangle = -i\sqrt{3}/4|\boxtimes\rangle$ . Hence  $\langle 0 | E_{123} | 0 \rangle \propto \langle \boxtimes | \boxtimes \rangle = 0$  in the fully symmetric phase and a similar computation in the dimer phase yields  $\langle 0 | E_{123} | 0 \rangle \simeq \langle \square | E_{123} | \square \rangle = 0$  as well. Thus there is no instability towards chiral symmetry breaking in our approach either, and we need to address the dynamics of  $E_{123}$ . Namely we compute the following dynamical correlation

$$\langle E_{123}(\omega) E_{123} \rangle = \sum_q |\langle q | E_{123} | 0 \rangle|^2 \delta(\omega - \epsilon_q + \epsilon_0) \quad (3)$$

where the sum runs over all eigenpairs  $\{\epsilon_q, |q\rangle\}_q$  of the impurity model (2). The above discussion shows that in the fully symmetric phase, the lowest pole in Eqn. 3 is located at the singlet gap energy  $\omega_1 = \epsilon_1 - \epsilon_0$  with weight  $Z_1 = |\langle 1 | E_{123} | 0 \rangle|^2 \simeq (\sqrt{3}/4)^2 |B \langle 1 | 0 \rangle_B|^2$ .

In Figure 2 we show the evolution of  $\omega_1$  and  $Z_1$  with increasing  $t_2/t_1$ . As expected, increasing the frustration  $t_2/t_1$  from  $t_2 = 0$  reduces  $\omega_1$  and increases  $Z_1$ , evidencing the enhancement of coherence of the three spins on a plaquette. In both paramagnetic phases the weight  $Z_1$  decreases very slowly, in the  $0.16 - 0.155$  range, showing that  $|B \langle 1 | 0 \rangle_B| \simeq 0.9$ . Hence, not only are the bath and the impurity weakly entangled, but also the bath states that accompany the lowest lying impurity states are quite

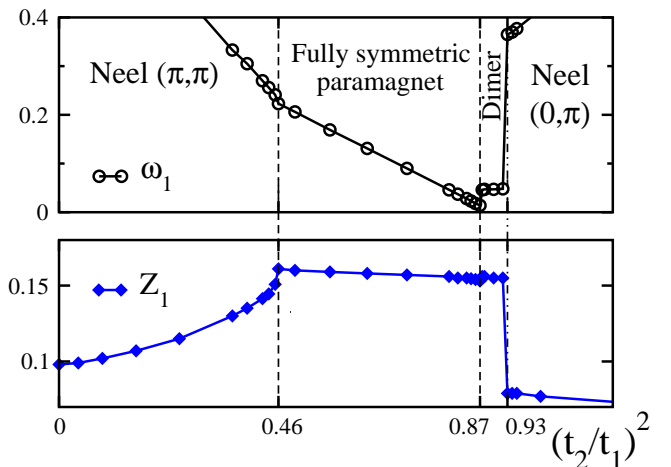


FIG. 2: (color online) Evolution of the frequency  $\omega_1$  and integrated weight  $Z_1$  of the lowest pole of the chiral correlation  $\langle E_{123}(\omega) E_{123} \rangle$  with increasing frustration.

similar. In the following, this will allow us to ignore the bath components of  $|0\rangle$  and  $|1\rangle$  temporarily. Although there is no significant “decoherence” induced by the coupling of the impurity to the bath, the bath does play a crucial role in determining the phase diagram: without it we would not be describing a system in the thermodynamic limit, able to sustain broken symmetry phases and transitions between them.

The upper panel of Figure 2 shows that for  $0.46 \lesssim (t_2/t_1)^2 \lesssim 0.87$ , the singlet gap  $\omega_1$  between  $|\boxtimes\rangle$  and  $|\boxtimes\rangle$  decrease linearly towards zero as  $(t_2/t_1)^2 \rightarrow 0.87$ . For comparison, the lowest pole of the cluster dynamical spin-spin correlations  $\langle m_{\mathbf{k}_1}(\omega) \cdot m_{-\mathbf{k}_1} \rangle$  is obtained for  $\mathbf{k}_1 = (\pi, \pi)$  in this region and yields a local estimate of the spin gap of about  $0.2 t_1$ .

In the fully symmetric phase, any combination  $|\Psi\rangle = a|\boxtimes\rangle + b|\boxtimes\rangle$  is not an eigenstate and instead has a dynamics with characteristic frequency  $\omega_1$ . As  $(t_2/t_1)^2 \rightarrow 0.87$ ,  $\omega_1 \rightarrow 0$  and all such states become eigenstates with zero-energy. This obviously includes chiral states, defined by  $\langle \Psi | E_{123} | \Psi \rangle \neq 0$ , and such that  $ba^* - ab^* \neq 0$ , but also the above-mentioned dimer states  $|\square\rangle$  and  $|\square\rangle$ , one of which will be eventually selected upon increasing  $t_2/t_1$  above 0.87.

We now ask whether these chiral and dimer states exhaust the possibilities of phases that can be described by plaquette DMFT and which compete near  $(t_2/t_1)^2 \simeq 0.87$ . One route consists in extending the above discussion of the chiral correlations. Namely we are looking for any additional hermitian operator  $A$  such that the correlation  $\langle A(\omega) A \rangle$  has its lowest pole at the energy of the singlet gap  $\omega_1$  in the fully symmetric phase. According to Eqn. 3 this translates as  $\langle 0 | A | 0 \rangle \simeq \langle \boxtimes | A | \boxtimes \rangle = 0$  and  $\langle 1 | A | 0 \rangle \simeq \langle \boxtimes | A | \boxtimes \rangle \neq 0$ . In

such a reduced subspace the possibilities are very limited: the set of  $2 \times 2$ , hermitian, off-diagonal matrices is exactly spanned by the two Pauli matrices  $\sigma_x, \sigma_y$ . In particular, the above computation of  $E_{123}$  can be recast in operator form as  $E_{123} = \sqrt{3}/4 \sigma_y$ . A similar computation for the dimerization operator  $D$  leads to  $D = \sqrt{3}/2 \sigma_x$ . In this synthetic form it is clear that we have exhausted the list of linearly independant operators whose fluctuations become infinitely soft at the transition point.

Interestingly, the local mean-field picture developed above allows us to further elaborate on the nature of the chiral phase that competes with the dimerized phase near  $(t_2/t_1)^2 \simeq 0.87$ . Indeed, repeating the above computation for all triplets of impurity sites leads to  $E_{123} = \sqrt{3}/4 \sigma_y = -E_{234} = E_{341} = -E_{412}$ . It is interesting to note the chiral spin liquid proposed by Wen in its large- $N$  treatment of the  $J_1 - J_2$  model obeys the same spatial symmetries. [14] Further, Wen derived both i) a chiral liquid and ii) a dimer solution of the mean-field equations. Both solutions were found to compete at large frustration  $J_2 \simeq J_1$ , although dimers are always energetically favored, in qualitative agreement with the present study.

*Conclusion* It is remarkable that a mean-field theory based on a plaquette is able to describe the phases of the  $J_1 - J_2$  model, as obtained within more exact approaches. [13, 16] The present study provides simple caricatures of the local aspects of these phases. Mean-field theory, however, does not contain the effects of long-wavelength fluctuations and is not expected to describe the location of the phase boundaries accurately. CDMFT also ignores more complicated forms of long-range order which cannot be tiled with impurities. Overall we expect that, upon increasing the size of the impurity, the phase boundaries in Figure 1 will shift, moving the paramagnetic region  $0.46 \lesssim (t_2/t_1)^2 \lesssim 0.93$  closer to the values of the nearby  $J_1 - J_2$  model, namely  $0.4 \lesssim J_2/J_1 \lesssim 0.6$ . [13] [16]. Nevertheless, we expect the local physics described in this paper to be robust and play an important role both at finite temperature and finite doping, which deserves further study within plaquette DMFT. In particular, doping this system in the region with low-lying chiral fluctuations may generate orbital currents or a  $d$ -density wave. Although no instability towards either of those orders was detected in the  $t_2 = 0$  case at finite doping, [17] the present study shows that this issue should be reconsidered for  $t_2 \neq 0$ .

On the experimental side, the search for physical realizations of a  $t_1 - t_2$  one-band Hubbard model resulted in materials with either small  $t_2/t_1$ , such as cuprates, which have  $(\pi, \pi)$  Néel-order at low-temperature, or very large  $t_2/t_1$ , such as  $\text{Li}_2\text{VOSiO}_4$ , lying well in the  $(0, \pi)$  Néel phase. [18, 19] However, the recently synthesized material  $\text{PbVO}_3$  [20] has intermediate frustration [21] and offers a possible realization of the non-magnetic phase described in this paper. In particular,

Raman scattering under pressure in various geometries should be able to probe for the low-lying chiral fluctuations [22, 23] and their evolution with frustration.

**ACKNOWLEDGEMENT:** This work was supported by the NSF under grant DMR No. DMR 0528969. Benoit Douçot, Olivier Parcollet, Marcello Civelli, Claire Lhuillier, Grégoire Misguich and Anne Passy are gratefully acknowledged for enlightening discussions.

---

\* Electronic address: domenge@physics.rutgers.edu

- [1] P. Anderson, Science **235**, 1196 (1987).
- [2] S. Sachdev and N. Read, Int. J. Mod. Phys B **5**, 219 (1991).
- [3] A. Georges, G. Kotliar, W. Krauth, and M. J. Rozenberg, Rev. Mod. Phys. **68**, 13 (1996).
- [4] G. Kotliar, S. Y. Savrasov, K. Haule, V. S. Oudovenko, O. Parcollet, and C. A. Marianetti, Rev. Mod. Phys. **78**, 865 (2006).
- [5] T. Maier, M. Jarrell, T. Pruschke, and M. H. Hettler, Rev. Mod. Phys. **77**, 1027 (2005).
- [6] A.-M. S. Tremblay, B. Kyung, and D. Sénéchal, Low Temperature Physics **32**, 424 (2006).
- [7] M. Civelli, M. Capone, S. S. Kancharla, O. Parcollet, and G. Kotliar, Phys. Rev. Lett. **95**, 106402 (2005).
- [8] T. D. Stanescu and G. Kotliar, Phys. Rev. B **74**, 125110 (2006).
- [9] B. Kyung and A. Tremblay, Phys. Rev. Lett. **97**, 046402 (2006).
- [10] A. Georges, R. Siddhartan, and S. Florens, Phys. Rev. Lett. **87**, 277203 (2001).
- [11] T. Ohashi, N. Kawakami, and H. Tsunetsugu, Phys. Rev. Lett. **97**, 066401 (2006).
- [12] J.-C. Domenge and G. Kotliar, in preparation.
- [13] G. Misguich and C. Lhuillier, in *Frustrated Spin Systems*, edited by H. T. Diep (World Scientific, Singapore, 2005).
- [14] X. G. Wen, F. Wilczek, and A. Zee, Phys. Rev. B **39**, 11413 (1989).
- [15] D. Poilblanc, E. Gagliano, S. Bacci, and E. Dagotto, Phys. Rev. B **43**, 10970 (1991).
- [16] A. H. Nevidomskyy, C. Scheiber, D. Sénéchal, and A.-M. S. Tremblay, Phys. Rev. B **77**, 064427 (2008).
- [17] A. Macridin, M. Jarrell, and T. Maier, Phys. Rev. B **70**, 113105 (2004).
- [18] R. Melzi, P. Carretta, A. Lascialfari, M. Mambrini, M. Troyer, P. Millet, and F. Mila, Phys. Rev. Lett. **85**, 1318 (2000).
- [19] G. Misguich, B. Bernu, and L. Pierre, Phys. Rev. B **68**, 113409 (2003).
- [20] R. Shpanchenko, V. Chernaya, A. Tsirlin, P. Chizhov, D. Sklovsky, E. Antipov, E. Khlybov, V. Pomjakushin, A. Balagurov, J. Medvedeva, et al., Chemistry of Materials **16**, 3267 (2004).
- [21] A. A. Tsirlin, A. A. Belik, R. V. Shpanchenko, E. V. Antipov, E. Takayama-Muromachi, and H. Rosner, Phys. Rev. B **77**, 092402 (2008).
- [22] B. S. Shastry and B. I. Shraiman, Phys. Rev. Lett. **65**, 1068 (1990).
- [23] P. E. Sulewski, P. A. Fleury, K. B. Lyons, and S.-W. Cheong, Phys. Rev. Lett. **67**, 3864 (1991).